2013

The optimisation of a turbulent swirl nozzle using CFD

Brett K. Thomas
Edith Cowan University

Zahir U. Ahmed
Edith Cowan University, z.ahmed@ecu.edu.au

Yasir M. Al-Abdeli
Edith Cowan University, y.al-abdeli@ecu.edu.au

Miccal T. Matthews
Edith Cowan University

Proceedings of the Australian Combustion Symposium
November 6-8, 2013, The University of Western Australia

The Optimisation of a Turbulent Swirl Nozzle Using CFD

Brett Thomas*, Zahir. U. Ahmed, Yasir M. Al-Abdeli, Miccal T. Matthews
School of Engineering
Edith Cowan University WA 6027 Australia

Abstract

Swirl is imparted into free and impinging nozzle flows as well as jet flames to affect convective heat transfer, fluid mixing or flame stability. At the nozzle exit plane, the emerging flow strongly influences downstream flow development and so factors which impact upon the emitted flow are worthy of study. This paper presents preliminary CFD analyses into the effect of design parameters and operational settings on the emerging flow at the exit plane for a swirl nozzle (Re_{max}~30,500). The research was conducted in the pre-manufacture stage to optimise the nozzle. Swirl is aerodynamically generated using multiple tangential ports located upstream of the exit plane and the streamwise flow is augmented with flow from two axial ports located at the nozzle base. Before reaching the exit plane, all flows pass through a contraction en route to a straight section of length (L). Factors studied in this paper include the angle of (inlet) tangential ports, the total length of the straight section (L), the ratio of axial-to-tangential inflows and the Reynolds number. Results show that larger tangential port angles and a shorter straight section help develop a modestly greater swirl number, but flows become less uniform as (L) is reduced. Swirl numbers only double if (tangential) inlet port flows are tripled.

Keywords: turbulent, swirl, nozzle, design optimisation, CFD.

1. Introduction

Compared to unconfined non-swirling jets, swirl generally yields larger jet spread and causes stronger centreline velocity decay and downstream vortex breakdown [1, 2]. In unconfined non-premixed flames, swirl affects stability characteristics [3] and steadiness [4]. However, with impingement studies, swirl inclusion has varied effects on heat transfer at the impingement surface with some [5, 6] reporting reduced heat transfer at impingement compared to non-swirling jets. The presence of a recirculating zone at the stagnation region has a similar effect [7]. Whilst this view is supported by some [8] who find no effects from swirl on the radial uniformity of impingement heat transfer, others suggest swirl has a positive influence on heat transfer [8-11], including improved uniformity [5, 12, 13]. In impinging flows, the variety of means used to impart swirl complicate this understanding of transition from non-swirling to swirling jets. Geometrically generated swirl has the potential to cause a dead-zone around the centerline and the jet may divert into multiple streams of flow before it impinges [11, 12, 14]. As a result, flow and heat transfer characteristics show drastically different results, even at no swirl, compared to conventional jets (pipe flow) [11, 13, 15]. Thus, aerodynamically generated swirl may facilitate insights into the transition from non-swirling-to-swirling jets, which is the focus of this study. With such diversity in reported outcomes and the realization that swirl flow uniformity (at the exit plane) affects downstream development, this study is part of a wider program into effects of swirl on heat transfer in turbulent impinging jets. In such studies, developing a swirl nozzle is first required but the effects of various design and operational parameters on the emerging flow are not always well understood. This paper presents computations to predict (pre-manufacture), the effects of various design constraints and operational parameters on flow development at the exit plane.

Swirl studies using RANS based simulations are available in literature [16-18]. The majority investigate the effects of flow parameters on flow characteristics and occurrence/stability of vortex breakdown, without considering the effects of design parameters on flow uniformity at the exit plane. Despite their relative simplicity, RANS approaches are in good agreement with experiments and capable of reproducing the steady-state flow-field of swirling jets at low swirl numbers [16-18], as applied in this study. Multiple expressions for swirl intensity are present [19] with swirl numbers usually defined based on the ratio of either the momentum or the velocity, of the tangential component to the axial component. Swirl intensity has also been expressed through the geometric properties [20]. In the present study, a dimensionless swirl number (S) is used and calculated via (1) as the ratio of the mean tangential velocity <W> to mean axial velocity <U>, both measured at the nozzle exit plane:

$$S = \frac{< W >}{< U >} \quad (1)$$

2. Methodology

Computational Fluid Dynamics (CFD) is used to optimise the swirl nozzle to analyse the effects of operational and design parameter changes on flows at the exit plane. To achieve this, COMSOL Multiphysics™ (v4.3) was deployed to single phase flows (air at 20°C, ref. pressure 1atm) which were solved in steady-state using the k-ε turbulent flow model (walls are assumed with no-slip). Figure 1 gives more details on the nozzle and the 3D fluid domain modelled. The effects of changing the axial-to-tangential inflows

* Corresponding author, Phone: (+61) 42 450 4920
Email: bthomas5@our.ecu.edu.au brett.thomas.eng@gmail.com

(section A[1] and T[2]), which varies the Reynolds number, and the angle of the tangential inlet ports (15° or 25°) as well as the downstream location of the contraction (section C[3]) from the exit plane (L=123 to 423mm) were all tested via CFD. Contractions are typically based on (internal) profiles which are known to produce exit velocities of non-uniformities of 2% (or less) and include the Batchelor-Shaw (BS) nozzle, the Cubic Equation (CE) contour nozzle and the ASME low and high beta nozzles [21]. In the nozzle designed, the CE contour was applied with length (75 mm) slightly less than twice the inner (cavity) diameter (40 mm). Flow rates imposed in the model have an upper value of 0.0148 m^3/s which reflects a peak delivery of 0.888 m^3/min. Table 1 presents the inflow conditions tested in the CFD simulations and the corresponding Reynolds numbers derived as:

$$\mathrm{Re} = \frac{< \mathrm{U} > \mathrm{D}}{\nu} = \frac{\mathrm{QD}}{\nu \mathrm{A}} \qquad (2)$$

In this regard, (D) is the inner nozzle diameter at the exit plane (40 mm), (Q) is the volume flow rate (m^3/s), (A) is the cross-sectional area at the exit plane (m^2), <U> is the bulk fluid velocity (m/s) and (ν) the kinematic fluid viscosity (1.51 x $10^{-5} m^2/s$). Table 1 also gives a breakdown of the combined flow across both axial ports (section A) and inflow at each tangential port (section T) as applied in the simulations. The ensuing results section presents the outcomes of CFD investigations to help identify the relative significance of modifying these various inflows on the swirl number formed at the exit plane. As shown in Fig. 1, in the fluid geometry developed, a rectangular co-ordinate system is used where the z-axis corresponds to the axial or streamwise direction (U). To obtain the tangential velocity component (W), the co-ordinate transformation for the velocity components was done as follows:

$$W = -V_X \sin\theta + V_Y \cos\theta \qquad (3)$$

where, V_X and V_Y are the velocities in the x- and y-directions in the Cartesian coordinate system, and the angle denoted by θ is defined as θ = atan (y/x) .

3. Results and Discussion

The study first determines the resulting swirl numbers if operational parameters, like the ratio of axial-to-tangential port inflows, change (pending experiments to validate). Such CFD predictions provide a valuable insight at the pre-manufacture stage. To achieve this, several ratios of axial-to-tangential flow rates are selected whereby total flows are proportioned from 0:100 (all streamwise flow via tangential ports which yields peak swirl number) to 100:0 (all the streamwise flow via axial ports which gives S=0). Figure 2 shows the results of this analysis and reveals a non-linear relationship between the ratio of axial-to-tangential inflow and swirl number.

The second aim is to study at the effects of design variations on the swirl number and flow uniformity at the exit plane and achieved by looking at two design parameters. Initially, the effects of changing the angle of tangential port entry was varied from 15° to 25° at the lowest Reynolds number (Re=10,000). This level of (Re) was selected in the simulations so as to see the effects on the minimal swirl number expected because it was believed that if a significant change in (S) resulted between 15° and 25°, then it is more than likely to also do so for higher Reynolds numbers. Figure 3 shows that varying (α) has minimal effect on (S). Secondly, the effect of changing the length of straight section (L) on (S) is analysed. This is an important consideration because although extending the length of straight sections may help ensure a fully developed turbulent pipe flow by the exit plane, additional lengths also imposes manufacturing costs and may lead to swirl decay. This analysis was done at Re= 30,543 as (S) developed at this level would likely constitute a peak value for the geometry and operational parameters tested. To change the value for (L), the nozzle was designed in a modular manner, whereby (L) could easily be varied by adding/removing sections (Fig. 1). Results for these simulations are presented in Fig. 4 and Fig. 5 and show that as the number of straight sections is reduced, (S) increases at the expense of flow uniformity. In relation to flow uniformity at the exit plane, the results show that a full-developed turbulent (pipe) flow, having a flatter central profile, is more likely to emerge at L=423 mm compared to lesser values. The minimal changes observed between L=323 mm and L=423 mm may also indicate a fully developed flow exists, in line with turbulent pipe flow theory and attaining fully developed flows after travelling a length of ~10 times the diameter at the entrance [35-37]. In our case the diameter, of relevance is the 40mm port opening at the end of the contraction (section C).

4. Conclusions

Swirl numbers (S) at the exit plane are a complex interaction of geometrical elements and operational parameters. Results demonstrate that CFD can be used to predict likely swirl numbers and flow uniformity. Further experimental results are needed to validate the predictions. The results also indicate the likely occurrence of a fully-developed turbulent (pipe) flow profile at exit and that using a 15° inclination angle is also sufficient and that no significant improvement in (S) is expected for 25°.

5. Acknowledgments

Brett Thomas did the CFD computations in his BEng (Mech) final year project. Zahir U. Ahmed is sponsored by the Dept. of Education, Employment and

[1] **Axial section (A):** In the physical nozzle, this includes a series of mesh screen and honeycombs to produce a more uniform velocity profile. In the CFD model, the top of section (A) forms an inlet port into the fluid domain and is assumed with a uniform velocity profile.

[2] **Tangential section (T)**: Imparts swirl into the flow via three circumferential ports angled at (α) and inclined 20° off the horizontal.

[3] **Contraction section (C):** This coalesces the tangential/axial flows.

Workplace Relations via an Endeavour Postgraduate Award.

6. References

1. Al-Abdeli, Y. M. and Masri, A. R., *Recirculation and flowfield regimes of unconfined non-reacting swirling flows.* Experimental Thermal and Fluid Science, 2003, **27**(5), p. 655-665.
2. Al-Abdeli, Y. M. and Masri, A. R., *Precession and recirculation in turbulent swirling isothermal jets.* Combustion Science and Technology, 2004, **176**(5-6), p. 645-665.
3. Al-Abdeli, Y. M. and Masri, A. R., *Stability characteristics and flowfields of turbulent non-premixed swirling flames.* Combustion Theory and Modelling, 2003, **7**(4), p. 731-766.
4. Al-Abdeli, Y. M. and Masri, A. R., Turbulent swirling natural gas flames: Stability characteristics, unsteady behavior and vortex breakdown. Combustion Science and Technology, 2007, **179**(1-2), p. 207-225.
5. Ward, J. and Mahmood, M. *Heat transfer from a turbulent, swirling, impinging jet*, in Heat transfer 1982; Proceedings of the Seventh International Conference, 1982, Munich, West Germany, p. 401-407.
6. Owsenek, B. L., Cziesla, T., Mitra, N. K., et al., *Numerical investigation of heat transfer in impinging axial and radial jets with superimposed swirl.* International Journal of Heat and Mass Transfer, 1996, **40**(1), p. 141-147.
7. Nozaki, A., Igarashi, Y. and Hishida, K., *Heat transfer mechanism of a swirling impinging jet in a stagnation region.* Heat Transfer—Asian Research, 2003, **32**(8), p. 663-673.
8. Wen, M. and Jang, K., *An impingement cooling on a flat surface by using circular jet with longitudinal swirling strips.* International Journal of Heat and Mass Transfer, 2003, **46**(24), p. 4657-4667.
9. Huang, L. and El-Genk, M. S., Heat transfer and flow visualization experiments of swirling, multi-channel, and conventional impinging jets. International Journal of Heat and Mass Transfer, 1998, **41**(3), p. 583-600.
10. Brown, K. J., Persoons, T. and Murray, D. B. *Heat transfer characteristics of swirling impinging jets*, in Proceedings of the International Heat Transfer Conference, 2010, Washington, DC, USA, p. 1-9.
11. Nuntadusit, C., Wae-hahyee, M., Bunyajitradulya, A., et al. *Heat transfer enhancement for a swirling jet impingement*, in ISFV14 - 14th International Symposium on Flow Visualization, 2010, EXCO Daegu, Korea, p. 1-9.
12. Bilen, K., Bakirci, K., Yapici, S., et al., *Heat transfer from a plate impinging swirl jet.* International Journal of Energy Research, 2002, **26**(4), p. 305-320.
13. Senda, M., Inaoka, K., Toyoda, D., et al., *Heat transfer and fluid flow characteristics in a swirling impinging jet.* Heat Transfer—Asian Research, 2005, **34**(5), p. 324-335.
14. Ianiro, A. and Cardone, G., *Heat transfer rate and uniformity in multichannel swirling impinging jets.* Applied Thermal Engineering, 2011, **49**, p. 89-98.
15. Lee, D. H., Won, S. Y. and Kim, Y. T., *Turbulent heat transfer from a fiat surface to a swirling round impinging jet.* International Journal of Heat and Mass Transfer, 2002, **45**, p. 223-227.
16. Guo, B., Fletcher, D. F., Marquez, G., et al. *RANS calculations and measurements of instabilities in swirl-stabilized jets and flames*, in 2003 Australian Symposium on Combustion & The 8th Australian Flames Days, 2003, Monash University, Australia.
17. Hoekstra, A. J., Derksen, J. J. and Van Den Akker, H. E. A., *An experimental and numerical study of turbulent swirling flow in gas cyclones.* Chemical Engineering Science, 1999, **54**, p. 2055-2065.
18. De Meester, R., Naud, B. and Merci, B. *Hybrid RANS/PDF calculations of Sydney swirling flames*, in Proceedings of the European Combustion Meeting, 2009, p. 1-6.
19. Toh, I., Honnery, D. and Soria, J., *Axial plus tangential entry swirling jet.* Experiments in Fluids, 2010, **48**(2), p. 309-325.
20. Alekseenko, S. V., Kuibin, P. A., Okulov, V. L., et al., *Helical vortices in swirl flow.* Journal of Fluid Mechanics, 1999, **382**, p. 195-243.
21. Hussain, A. and Ramjee, V., *Effects of the axisymmetric contraction shape on incompressible turbulent flow*. American Society of Mechanical Engineers, 1975, **1**.

Table 1. Inflow conditions imposed in the CFD simuations.

Exit Plane Diameter, **D** (m)	Exit Plane Area, **A** (m^2)	Kinematic Viscosity, **ν** (m^2/s)	Bulk Velocity, **v** (m/s)	Volume Flow Rate, **Q** (m^3/s)	Reynolds Number
0.04	0.00126	0.0000151	3.78	0.00474	Re1 = 10000
			7.55	0.00949	Re2 = 20000
			11.53	0.0148	Re3 = 30543

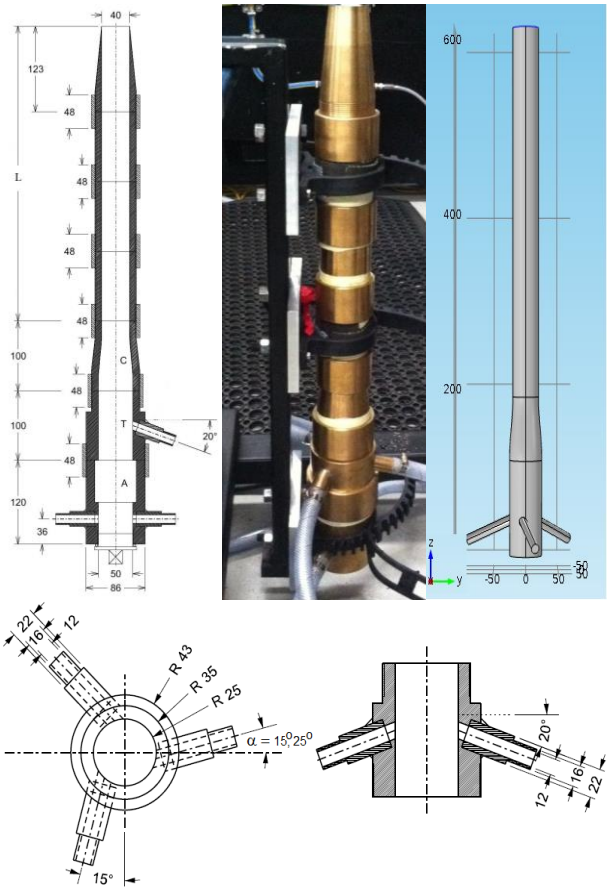

Figure 1. Nozzle dimensions (top - left) and the length of the straight section which was varied (L=123mm - 423mm). Also shown is the final manufactured nozzle (top centre), the fluid domain modeled using CFD (top right) and the angle of tangential ports which was varied (bottom left, α=15 °or 25°). The port inclination off the horizontal (bottom right) was always 20°. Images not to scale.

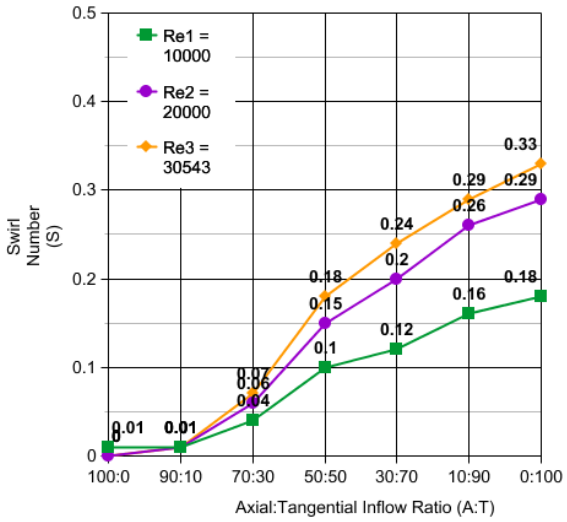

Figure 2. Predicted swirl numbers at different ratios of axial-to-tangential port inflows for Re=10,000 to 30,543 (Length L = 423mm).

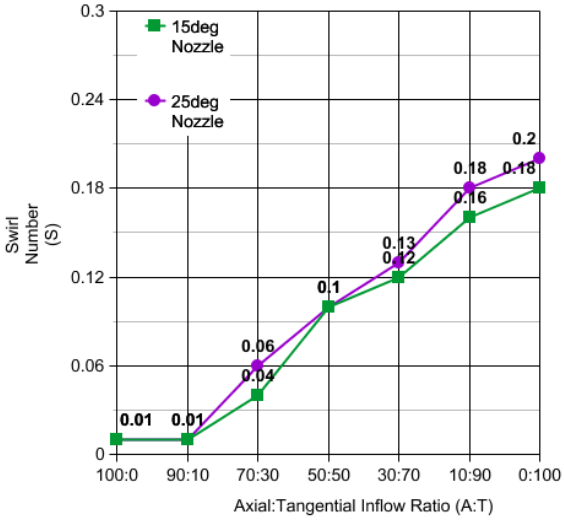

Figure 3. Predicted swirl numbers at different orientations of tangential ports for Re=10,000 (Length L = 423mm).

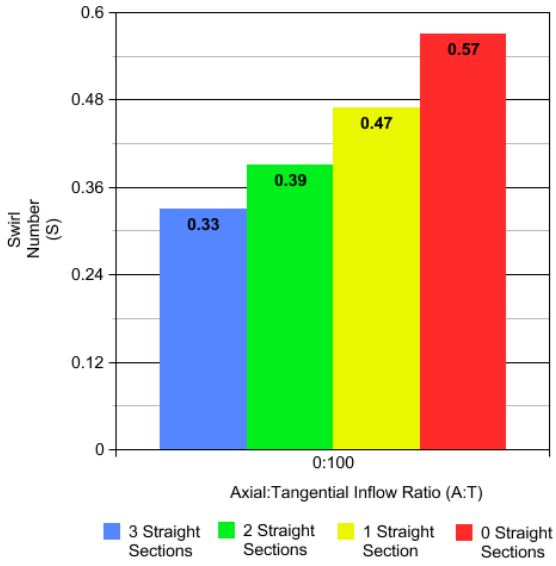

Figure 4. Predicted swirl numbers at different lengths upstream of the exit plane for Re=30,543 (L=123 for 0 strraight sections, L=223 for 1 straight section, L=323 for 2 straight sections and L = 423mm for 3 straight sections). Fig 1 shows dimension L.

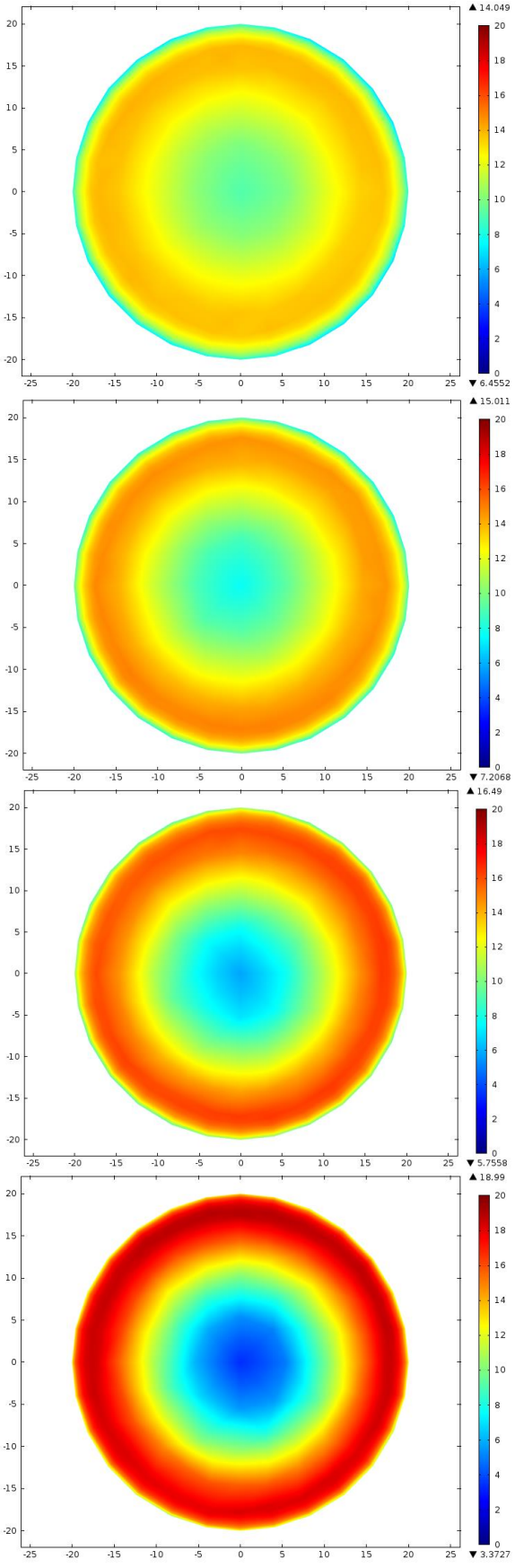

Figure 5. The effects of changing straight section length on the uniformity of velocity magnitude at the exit plane for Re = 30,543 and axial-to-tangential flow = 0:100. (From the top: L = 423mm, L = 323mm, L = 223mm, L = 123mm)